JACS
JOURNAL OF THE AMERICAN CHEMICAL SOCIETY

Communication

pubs.acs.org/JACS

Fluorogenic Azidofluoresceins for Biological Imaging

Peyton Shieh,[†,∥] Matthew J. Hangauer,[†,∥,⊥] and Carolyn R. Bertozzi*[,†,‡,§]

[†]Departments of Chemistry and [‡]Molecular and Cell Biology and [§]Howard Hughes Medical Institute, University of California, Berkeley, California 94720, United States

Supporting Information

ABSTRACT: Fluorogenic probes activated by bioorthogonal chemical reactions can enable biomolecule imaging in situations where it is not possible to wash away unbound probe. One challenge for the development of such probes is the a priori identification of structures that will undergo a dramatic fluorescence enhancement by virtue of the chemical transformation. With the aid of density functional theory calculations reported previously by Nagano and co-workers, we identified azidofluorescein derivatives that were predicted to undergo an increase in fluorescence quantum yield upon Cu-catalyzed or Cu-free cycloaddition with linear or cyclic alkynes, respectively. Four derivatives were experimentally verified in model reactions, and one, a 4-azidonaphthylfluorescein analogue, was further shown to label alkyne-functionalized proteins in vitro and glycoproteins on cells with excellent selectivity. The azidofluorescein derivative also enabled cell imaging under no-wash conditions with good signal above background. This work establishes a platform for the rational design of fluorogenic azide probes with spectral properties tailored for biological imaging.

Bioorthogonal chemistry has enabled the visualization and study of biomolecules that cannot be tagged with genetically encoded fluorescent proteins.[1] Much work has been devoted to expanding the toolbox of bioorthogonal reactions, and these efforts can be complemented by the development of fluorogenic probes.[2] Such probes are typically endowed with a functionality that suppresses fluorescence. Its transformation during the reaction creates a new functionality that no longer quenches the fluorescence of the underlying system, resulting in a fluorescence enhancement. Such probes offer significant advantages for imaging studies in which it is not possible to wash away unreacted probe, such as real-time imaging of dynamic processes in cells or visualization of molecules in live organisms.

One of the most widely used bioorthogonal reactions is the azide−alkyne [3 + 2] cycloaddition to form a triazole. This reaction has enabled the selective visualization of azide- or alkyne-labeled proteins, glycans, nucleic acids, and lipids.[3] Several azide-[4−7] and alkyne-functionalized[7−11] fluorogenic probes have been reported, largely based on coumarins,[4,8] naphthalimides,[7] and other systems that require UV excitation and emit blue light.[5,10,11] Such wavelengths are not ideal for biological imaging because of high levels of autofluorescence and poor tissue penetrance.[13]

An obvious improvement upon these designs would be the development of azido or alkynyl fluorogenic probes with longer excitation and emission wavelengths. Some attempts at achieving this goal have been made. Recently, an azido-BODIPY probe was reported, but the compound was unstable and unable to react specifically with alkynes on cellular biomolecules.[6] An alkynylbenzothiazole analogue emitting at ∼500 nm was reported, but its fluorescence enhancement upon reaction with azides was a modest 3.5-fold in aqueous buffer.[11] A screen of 200 combinations of various alkynylxanthenes and organic azides produced two reagent pairs that reacted to give a 10-fold fluorescence enhancement in an organic solvent.[12] The utility of these alkyne/azide pairs in biological settings remains unclear. Thus, fluorogenic azido or alkynyl probes that perform well as cell-imaging reagents remain an important goal.

Here we report the rational design and experimental validation of azide-functionalized fluorogenic probes based on the widely used blue-excitation/green-emission fluorescein scaffold. Our design capitalizes on a theoretical model developed by Nagano and co-workers that enables the prediction of fluorescence quantum yields based on density functional theory calculations.[14] Nagano demonstrated that the pendant aryl ring of fluorescein can quench fluorescence via photoinduced electron transfer.[15] This quenching can be increased or decreased in a predictable manner by altering the electron density of the aryl ring using various substituents. More importantly, Nagano and co-workers also demonstrated a direct relationship between the experimentally determined fluorescence quantum yield and the calculated energy of the highest occupied molecular orbital (E_{HOMO}) of the pendant aryl ring at the B3LYP/6-31G(d) level of theory. Thus, in principle, by calculating the E_{HOMO} value of the aryl ring, one can predict the fluorescence quantum yield of the corresponding fluorescein and identify suitable targets for experimental evaluation. This insight has guided the design of other activatable fluorescein-based probes.[16,17]

Applying this concept to the development of a fluorogenic azidofluorescein, we performed computational analyses of a panel of fluorescein analogues in which the azide group was directly appended to a variety of aryl substituents [Table S1 in the Supporting Information (SI)]. We anticipated that triazole formation would lower the aryl E_{HOMO} value relative to that of the azide-functionalized substrate, reducing photoinduced electron transfer and resulting in fluorescence turn-on (Figure 1). We focused our analysis on targets that could be readily synthesized from commercially available bromo- or iodoaryl

Received: August 17, 2012
Published: October 1, 2012

dx.doi.org/10.1021/ja308203h | J. Am. Chem. Soc. 2012, 134, 17428−17431

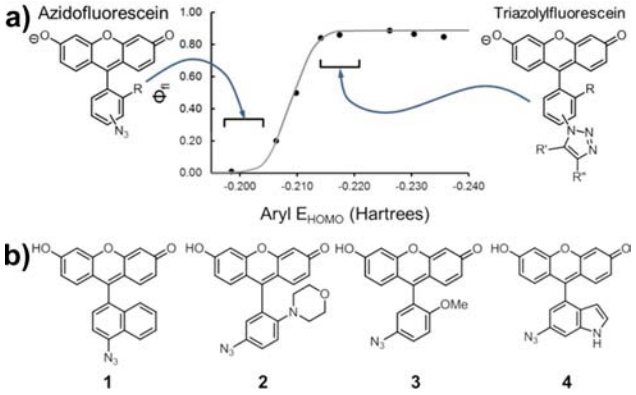

Figure 1. Computation-aided design of fluorogenic azidofluorescein analogues. (a) Relationship between E_{HOMO} of the pendant aryl group and the fluorescence quantum yield. The ideal E_{HOMO} values of the azido- and triazolylfluorescein analogues (left and right, respectively) are indicated with brackets.[14] (b) Structures of target azidofluoresceins **1**–**4**.

starting materials with a substituent ortho to the halogen.[18] Table S1 shows the 15 analogues chosen for computational studies as well as the E_{HOMO} values of the aryl azides and corresponding triazoles calculated at the B3LYP 6-31G(d) level of theory.

Calculations indicated that, with one exception, all of the compounds should exhibit the expected decrease in the aryl E_{HOMO} value upon triazole formation. Four of the compounds (**1**–**4**; Figure 1b) were chosen as targets for synthesis and further evaluation. These candidates possessed azide E_{HOMO} values of −0.196 to −0.210 hartree and triazole E_{HOMO} values of −0.203 to −0.220 hartree. Given the relationship between the fluorescence quantum yield and E_{HOMO}, we anticipated that **1**–**4** would exhibit an increase in fluorescence quantum yield upon triazole formation at pH 7.4.[19]

Compounds **1**–**3** were prepared by addition of the corresponding aryllithium compound to a protected xanthone derivative, an approach reported previously by Tsien and co-workers (Scheme 1).[22] To generate **1**, we subjected

Scheme 1. Synthesis of Azidofluorescein 1

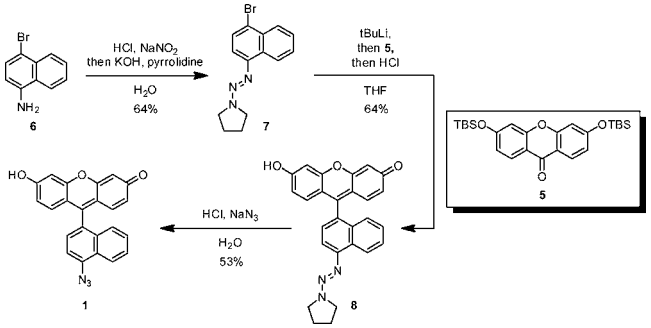

commercially available bromoaniline **6** to diazotization and then protected the diazonium group by reaction with pyrrolidine,[20,21] affording aryl triazene **7**, which underwent lithium–halogen exchange and addition to bis-*tert*-butyldimethylsilyl (TBS)-protected xanthone **5**[22] to afford fluorescein derivative **8**. Treatment of **8** with acid unmasked the diazonium group, which was displaced by azide anion to afford **1**. Azidofluoresceins **2** and **3** were prepared using the same strategy (see the SI). Attempts to convert 4-bromo-6-aminoindole, the starting material for compound **4**, to the corresponding triazene were unsuccessful.[23] Instead, we opted to start from acetylated indole **10**, which was prepared from the known compound **9** by iron reduction and acetylation in acetic acid (Scheme 2). In one pot, we treated **10** with 2 equiv of

Scheme 2. Synthesis of Azidofluorescein 4

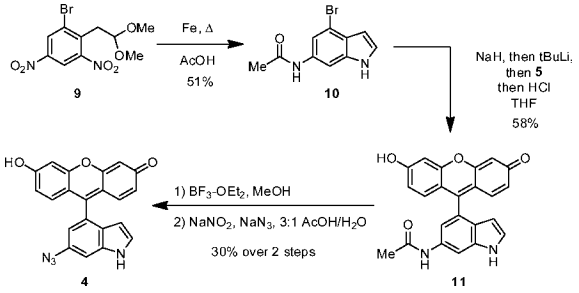

sodium hydride and then with *tert*-butyllithium to effect lithium–halogen exchange; coupling with **5** afforded **11** after acid workup. Deacetylation using $BF_3{\cdot}OEt_2$ in MeOH,[24] diazotization, and azide displacement then afforded **4**.

To synthesize the triazole products for photophysical measurements, **1**–**4** were further reacted with model alkynes **12**, **13** (DIFO), and **14** (DIMAC) (Figure 2) under Cu-

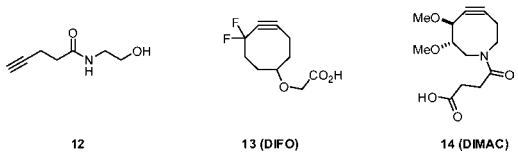

Figure 2. Alkynes used for triazolylfluorescein synthesis.

catalyzed (for **12**) or Cu-free (**13** and **14**) conditions.[25,26] The fluorescence quantum yields of all of these compounds were then measured in pH 7.4 phosphate-buffered saline (PBS) (Table 1).[27] Each triazolylfluorescein showed an increase in fluorescence quantum yield relative to the parent azidofluorescein. The relationship between the fluorescence quantum yield and the calculated E_{HOMO} followed a trend similar to that observed by Nagano[14] (Figure 3). As a point of comparison, we analyzed the known compound 5-azidofluorescein (N_3-fluor), which is currently used as an alkyne-specific probe but has not been reported to be fluorogenic.[28,29] The calculated E_{HOMO} values of N_3-fluor and its corresponding triazole product with **12** were −0.242 and −0.246 hartree, respectively, suggesting that both compounds should be highly fluorescent. Consistent with this prediction, we found the two compounds to have fluorescent quantum yields of 0.75 and 0.59, respectively (Table 1).

Interestingly, the fluorescence enhancement of **1**–**4** upon triazole formation was dependent on the structure of the alkyne substrate, but not in a systematic way. Presumably, structure-dependent pathways for nonradiative decay contribute to the observed fluorescence of the triazole products. Nonetheless, half of the azidofluorescein–alkyne pairs gave a >10-fold fluorescence turn-on, indicating that rational design principles can more efficiently identify fluorogenic reagent pairs than undirected screening approaches.

dx.doi.org/10.1021/ja308203h | J. Am. Chem. Soc. 2012, 134, 17428–17431

Table 1. Fluorescence Properties of Azido- and Triazolylfluoresceins[a]

compound	λ_{ex} (nm)	λ_{em} (nm)	Φ_{500}	increase
fluorescein	490	510	–	–
1	497	513	0.024	–
1–**12**	495	518	0.70	29×
1–DIFO	499	517	0.81	34×
1–DIMAC	499	517	0.72	30×
2	501	521	0.00056	–
2–**12**	506	517	0.0018	3.2×
2–DIFO	507	522	0.0018	3.2×
2–DIMAC	507	521	0.00076	1.4×
3	496	516	0.057	–
3–**12**	499	520	0.72	13×
3–DIFO	499	519	0.49	8.6×
3–DIMAC	499	518	0.72	13×
4	497	518	0.0052	–
4–**12**	499	519	0.13	25×
4–DIFO	497	520	0.019	3.7×
4–DIMAC	497	516	0.020	3.8×
N_3-fluor	492	511	0.75	–
N_3-fluor–**12**	494	516	0.59	0.79×

[a] Measured in pH 7.4 PBS. "**1**–**12**" denotes the triazolylfluorescein product of the reaction between **1** and **12**. Other triazolylfluoresceins are named analogously.

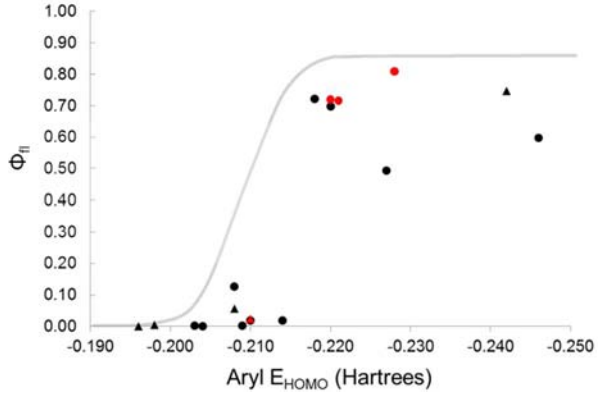

Figure 3. Relationship between the calculated E_{HOMO} of the pendant aryl group and the fluorescence quantum yield (Φ_{fl}) for a series of azidofluoresceins and triazolylfluoresceins. The gray line denotes the relationship between E_{HOMO} and Φ_{fl} determined in ref 14. Points represent experimental data for individual azidofluoresceins (▲) and triazolylfluoresceins (●). The points corresponding to **1** and its triazole products are highlighted in red.

Of the azidofluoresceins tested, **1** gave the highest and most alkyne-independent increase in fluorescence quantum yield at pH 7.4. Thus, we chose to evaluate its use further in biological labeling. First, we performed a model reaction with alkyne **12** under standard biological labeling conditions ($CuSO_4$, ligand,[30,31] and sodium ascorbate). The expected fluorescence increase was observed, and the reaction was complete within 1 h (Figure S2 in the SI). We next demonstrated that **1** can selectively label alkyne-tagged proteins. Bovine serum albumin (BSA) was functionalized with alkynes by modification of its lysine side chains with 4-pentynoyl *N*-hydroxysuccinimide (NHS) ester. An alkene-modified control sample was produced by reacting BSA with 4-pentenoyl-NHS ester. Alkyne- and alkene-modified BSA as well as unmodified BSA were incubated with **1**, $CuSO_4$, TBTA, and sodium ascorbate in 95:5 PBS (pH 7.4)/*tert*-butyl alcohol, and the samples were analyzed by SDS-PAGE. Fluorescence scanning showed that only alkyne-modified BSA was chemically labeled and that the labeling occurred in a Cu-dependent manner (Figure S3).

To evaluate azidofluorescein **1** as a biological imaging reagent, Chinese hamster ovary (CHO) cells were metabolically labeled with 50 μM peracetylated *N*-(4-pentynoyl)-mannosamine (Ac_4ManNAl) for 3 days as previously described.[32] These cells convert Ac_4ManNAl to the corresponding alkynylsialic acid, which is then incorporated into cell-surface glycoproteins. Control cells were incubated with peracetylated *N*-acetylmannosamine (Ac_4ManNAc). The cells were then fixed with paraformaldehyde and incubated with **1**, $CuSO_4$, sodium ascorbate, and TBTA for 1 h. After washing, the cells showed robust alkyne-dependent labeling with **1** (Figure S4). The experiment was then repeated, but without the washing step after reaction with **1**. As shown in Figure 4,

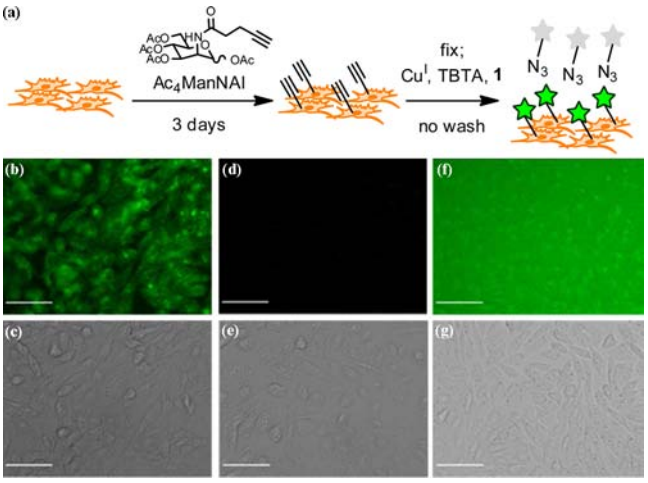

Figure 4. No-wash cell labeling with azidofluorescein probes. (a) Outline of the no-wash labeling experiment using Ac_4ManNAl and **1**. CHO cells were metabolically labeled with Ac_4ManNAl or Ac_4ManNAc for 3 days and then then reacted for 1 h with 25 μM probe as well as the other reagents for Cu-catalyzed click chemistry. (b–g) Fluorescence images (top row) and corresponding differential interference contrast images (bottom row): (b, c) Ac_4ManNAl-treated cells reacted with **1**; (d, e) Ac_4ManNAc-treated cells reacted with **1**; (f, g) Ac_4ManNAl-treated cells reacted with N_3-fluor. Scale bars = 50 μm. Exposure time/fluorescence cutoffs were (b, d) 150 ms/150–400 nm and (f) 10 ms/500–900 nm.

bright cell-surface fluorescence was observed for alkyne-labeled cells (Figure 4b) relative to the background observed with the control (Ac_4ManNAc-labeled) cells (Figure 4d). In contrast, whereas nonfluorogenic N_3-fluor also labels cells in an alkyne-dependent manner (Figure S5), the strong fluorescence signal of this azide dye gave a high background under no-wash conditions (Figure 4f), thereby obscuring the cell-surface labeling of alkynyl sugars.

A potential problematic side reaction of aryl azides is their reduction to the corresponding anilines by endogenous thiols. This reaction has been demonstrated to proceed under physiological conditions,[33] and indeed, it has undermined the use of azidonaphthalimides as biological imaging reagents.[7] Aryl azide reduction has also been used to detect intracellular hydrogen sulfide.[34] Calculations indicate that this reduction pathway would not be an issue for **1**, as the predicted aryl

dx.doi.org/10.1021/ja308203h | J. Am. Chem. Soc. 2012, 134, 17428–17431

E_{HOMO} value of the aniline reduction product is higher than that of the starting aryl azide (−0.189 vs −0.210 hartree). To demonstrate this experimentally, we reduced **1** with dithiothreitol and measured the fluorescence quantum yield of the arylamine product. As expected, reduction resulted in a decrease in the fluorescence quantum yield from 0.024 to 0.0067 at pH 7.4, indicating that if this side reaction were to occur in vivo, it would not contribute significantly to the background fluorescence.

In summary, by taking advantage of the observed relationship between E_{HOMO} of a pendant aryl substituent and the fluorescence quantum yield, we were able to identify potential fluorogenic azidofluoresceins. One of these, **1**, was suitable for no-wash imaging of cells. This compound is cell-permeable and may be suitable for intracellular imaging of biomolecule-associated cyclooctynes as well (Figure S6). We anticipate that this general strategy will also be useful for the development of fluorogenic alkynylfluorescein analogues. Indeed, calculations indicated that conversion of aryl alkynes to the corresponding triazoles results in a significant increase in E_{LUMO}. In principle, alkynylfluoresceins that are internally quenched by photoinduced electron transfer, in this case from the xanthene to the aryl ring, should undergo fluorescence enhancement upon triazole formation.[35] This notion, as well as the extension of the design principle to red-shifted fluorophores, are interesting future directions.

■ ASSOCIATED CONTENT

Supporting Information

Experimental and synthetic procedures, materials, and supporting figures and tables. This material is available free of charge via the Internet at http://pubs.acs.org.

■ AUTHOR INFORMATION

Corresponding Author

crb@berkeley.edu

Present Address

[⊥]School of Medicine, University of California, San Francisco, CA 94143.

Author Contributions

[‖]P.S. and M.J.H. contributed equally.

Notes

The authors declare no competing financial interest.

■ ACKNOWLEDGMENTS

This work was funded by NIH Grant GM58867 to C.R.B. We thank Prof. C. Chang (UC Berkeley) for the generous use of his fluorimeter. M.J.H. was supported by a National Defense Science and Engineering Graduate Fellowship.

■ REFERENCES

(1) For a general review of bioorthogonal chemistry, see: Sletten, E. M.; Bertozzi, C. R. *Angew. Chem., Int. Ed.* **2009**, *48*, 6974.

(2) For a review of fluorogenic click probes, see: Le Droumaguet, C.; Wang, C.; Wang, Q. *Chem. Soc. Rev.* **2010**, *39*, 1233.

(3) For reviews of applications of the azide−alkyne [3 + 2] cycloaddition in chemical biology, see: Best, M. D. *Biochemistry* **2009**, *48*, 6571. Jewett, J. C.; Bertozzi, C. R. *Chem. Soc. Rev.* **2010**, *39*, 1272.

(4) Sivakumar, K.; Xie, F.; Cash, B. M.; Long, S.; Barnhill, H. N.; Wang, Q. *Org. Lett.* **2004**, *6*, 4603.

(5) Xie, F.; Sivakumar, K.; Zeng, Q. B.; Bruckman, M. A.; Hodges, B.; Wang, Q. *Tetrahedron* **2008**, *64*, 2906.

(6) Wang, C.; Xie, F.; Suthiwangcharoen, N.; Sun, J.; Wang, Q. *Sci. China: Chem.* **2012**, *55*, 125.

(7) Sawa, M.; Hsu, T. L.; Itoh, T.; Sugiyama, M.; Hanson, S. R.; Vogt, P. K.; Wong, C. H. *Proc. Natl. Acad. Sci. U.S.A.* **2006**, *103*, 12371.

(8) Zhou, Z.; Fahrni, C. J. *J. Am. Chem. Soc.* **2004**, *126*, 8862.

(9) Jewett, J. C.; Bertozzi, C. R. *Org. Lett.* **2011**, *13*, 5937.

(10) Key, J. A.; Cairo, C. W. *Dyes Pigm.* **2010**, *88*, 95.

(11) Qi, J.; Han, M.-S.; Chang, Y.-C.; Tung, C.-H. *Bioconjugate Chem.* **2011**, *22*, 1758.

(12) Li, J.; Hu, M.; Yao, S. Q. *Org. Lett.* **2009**, *11*, 3008.

(13) Weissleder, R.; Ntziachristos, V. *Nat. Med.* **2003**, *9*, 123.

(14) Urano, Y.; Kamiya, M.; Kanda, K.; Ueno, T.; Hirose, K.; Nagano, T. *J. Am. Chem. Soc.* **2005**, *127*, 4888.

(15) Miura, T.; Urano, Y.; Tanaka, K.; Nagano, T.; Ohkubo, K.; Fukuzumi, S. *J. Am. Chem. Soc.* **2003**, *125*, 8666.

(16) Kamiya, M.; Kobayashi, H.; Hama, Y.; Bernardo, M.; Nagano, T.; Choyke, P. L.; Urano, Y. *J. Am. Chem. Soc.* **2007**, *129*, 3918.

(17) Kobayashi, T.; Urano, Y.; Kamiya, M.; Ueno, T.; Kojima, H.; Nagano, T. *J. Am. Chem. Soc.* **2007**, *129*, 6696.

(18) This ortho substituent restricts the rotation around the C_{aryl}−C_{aryl} bond and is necessary for maintaining predictable fluorescence quantum yields.[14]

(19) Nagano and co-workers[14] have shown that while the general trends relating E_{HOMO} to the quantum yield at different pH values are similar, the exact E_{HOMO} values at which the fluorescence dramatically increases are pH-dependent. We performed our calculations with the anionic form of fluorescein, which should predominate at physiological pH.

(20) Gross, M. L.; Blank, D. H.; Welch, W. M. *J. Org. Chem.* **1993**, *58*, 2104.

(21) Liu, C. Y.; Knochel, P. *J. Org. Chem.* **2007**, *72*, 7106.

(22) Mintaz, A. K.; Kao, J. P. Y.; Tsien, R. Y. *J. Biol. Chem.* **1989**, *265*, 8171.

(23) For another example of an unsuccessful attempt at triazene formation from aminoindoles, see: Cirrincione, G.; Almerico, A. M.; Dattolo, G.; Aiello, E.; Diana, P.; Grimaudo, S.; Barraja, P.; Mingoia, F.; Gancitano, R. A. *Eur. J. Med. Chem.* **1994**, *29*, 889.

(24) Miltsov, S.; Rivera, L.; Encinas, C.; Alonso, J. *Tetrahedron Lett.* **2003**, *44*, 2301.

(25) Baskin, J. M.; Prescher, J. A.; Laughlin, S. T.; Agard, N. J.; Chang, P. V.; Miller, I. A.; Lo, A.; Codelli, J. A.; Bertozzi, C. R. *Proc. Natl. Acad. Sci. U.S.A.* **2007**, *104*, 16793.

(26) Sletten, E.; Bertozzi, C. R. *Org. Lett.* **2008**, *10*, 3097.

(27) The values we measured were on average lower than Nagano's trend would predict. We considered whether measurements at pH 13, as performed by Nagano, would reconcile the observed differences, but for the most part, the fluorescence quantum yields of **1**−**4** were unchanged at higher pH.

(28) Rotman, A.; Heldman, J. *Biochemistry* **1981**, *20*, 5995.

(29) Salic, A.; Mitchison, T. J. *Proc. Natl. Acad. Sci. U.S.A.* **2008**, *105*, 2415.

(30) Hong, V.; Steinmetz, N. F.; Manchester, M.; Finn, M. G. *Bioconjugate Chem.* **2010**, *21*, 1912.

(31) Besanceney-Webler, C.; Jiang, H.; Zheng, T.; Feng, L.; Soriano del Amo, D.; Wang, W.; Klivansky, L. M.; Marlow, F. L.; Liu, Y.; Wu, P. *Angew. Chem., Int. Ed.* **2011**, *50*, 8051.

(32) Hsu, T.-L.; Hanson, S. R.; Kishikawa, K.; Wang, S.-K.; Sawa, M.; Wong, C.-H. *Proc. Natl. Acad. Sci. U.S.A.* **2007**, *104*, 2614. Chang, P. V.; Chen, X.; Smyrniotis, C.; Xenakis, A.; Hu, T. S.; Bertozzi, C. R.; Wu, P. *Angew. Chem., Int. Ed.* **2009**, *48*, 4030.

(33) Staros, J. V.; Bayley, H.; Standring, D. N.; Knowles, J. R. *Biochem. Biophys. Res. Commun.* **1978**, *80*, 568.

(34) Lippert, A. R.; New, E. J.; Chang, C. J. *J. Am. Chem. Soc.* **2011**, *133*, 10078. Peng, H.; Chen, S.; Chen, Z.; Ren, W.; Ai, H. *J. Am. Chem. Soc.* **2012**, *134*, 9589.

(35) Mineno, T.; Ueno, T.; Urano, Y.; Kojima, H.; Nagano, T. *Org. Lett.* **2006**, *8*, 5963.